

DEVELOPMENT OF A CLOSED-LOOP CONTROL SYSTEM FOR CONTACT TIP TO WORK DISTANCE AND INTERPASS TEMPERATURE IN WIRE ARC ADDITIVE MANUFACTURING OF ARCHITECTURAL FACADES

Y. Yamagata*, T. Sagawa*, S. Aoki*, T. Abe†, and J. Kaneko†

*Institute of Technology, Shimizu Corporation, Japan

†Division of Mechanical Engineering and Science, Saitama University, Japan

Abstract

This study introduces a closed-loop control system for Contact Tip to Work Distance (CTWD) and interpass temperature in Wire Arc Additive Manufacturing (WAAM), aimed at enhancing the production of architectural facades. By integrating feedback from laser-profiled measurements and thermographic cameras, the system dynamically adjusts CTWD and temperature settings, addressing the challenges of inconsistency in layer deposition and thermal accumulation. The implementation of this system enabled the automated manufacturing of aluminum mullion with a height of 855 mm. Trials confirmed the system's ability to maintain consistent layer quality and thickness distribution, while effectively preventing defects such as voids. The results demonstrate that precise control of CTWD and interpass temperature is crucial for optimizing the quality and reproducibility of WAAM components, making it a valuable advancement for the construction industry in customizing large-scale metal structures.

1. Introduction

Over the past decades, a computation-based approach to design has developed [1] and become popular among architects and designers. Such computational design approaches rely on trial and error via programming to derive optimal shapes. However, the resulting optimal shapes can be too complex to be realized through traditional manufacturing processes like machining or casting. As a result, Additive Manufacturing (AM), particularly known for its high shape-making freedom, has gained attention in the construction industry [2], [3]. Among the metal AM technologies used in construction, Wire Arc Additive Manufacturing (WAAM) stands out [4], [5], [6]. WAAM involves melting the base material with an arc discharge to form a molten pool, into which wire fed from a torch is melted and deposited [7]. WAAM is superior to other metal AM technologies in terms of deposition speed, cost, and mechanical properties [8], making it suitable for medium to large-scale parts [9]. Therefore, the compatibility of WAAM with the construction industry is enhanced due to its suitability for producing large-scale components at a lower cost.

The construction industry is exploring the use of WAAM technology for facade manufacturing [10]. Facades, which form the entrances of buildings, require high aesthetics and are suitable for the shape freedom offered by AM technologies. In this study, we focus on mullions, commonly used in facades [11], as our fabrication target. Mullions are vertical dividers such as those supporting glass, as shown in Figure 1. The characteristics of mullions include lengths of 3-5 meters, typical of building sizes, and commonly use aluminum materials. When fabricating such elongated structures using WAAM, two main challenges arise. The first challenge is controlling the Contact Tip to Work Distance (CTWD), which refers to the distance between the contact tip

and the workpiece, as illustrated in Figure 2. Too short a CTWD can lead to interference between the torch and workpiece or burn-back issues, complicating continuous deposition. Conversely, too long a CTWD can result in insufficient coverage by the shielding gas and the formation of black oxides due to the Mg content in Al-Mg materials [12]. Therefore, maintaining a consistent CTWD during deposition is necessary. However, the conditions of heat input and dissipation during deposition are not constant, making it difficult to predict the actual height of the layer. Thus, the higher the workpiece, the more likely the CTWD is to deviate from the target. To address this issue, attempts have been made to measure CTWD and maintain it at a constant level using closed-loop control. Methods for measuring CTWD can be broadly categorized into two types: those that use process signals and those that employ external sensors. One method using process signals involves detecting CTWD by measuring short-circuit resistance [13]. However, this approach is difficult when depositing aluminum, which has a lower resistivity compared to other metals. As for methods utilizing external sensors, a technique that employs a welding visualization camera has been proposed [14]. However, due to its reliance on image processing, achieving accurate measurements is challenging. Therefore, this study adopts a laser profiler as a more precise method for measuring CTWD. A laser profiler is a device that projects a band of laser light onto the surface of an object and measures changes in the reflected light using a CMOS sensor. This allows for non-contact measurement of cross-sectional features such as height, thickness, and steps. It excels compared to other methods due to its ability to acquire shape data with a high precision of approximately 1.0 μm . It also offers the advantage of simultaneously capturing both height and thickness data. This advantage becomes especially important as the size of the fabricated objects increases, since it becomes difficult to capture shape data after fabrication using methods like X-ray Computed Tomography (CT) scanning. Being able to measure both height and thickness during the process offers a clear advantage over other CTWD measurement methods, such as those that use current, voltage, wire feed speed, microphones, or spectrometers [15], which can only measure height. However, since it is necessary to control the sensor orientation to measure thickness, this study proposes a control method that utilizes a positioner table to enable measurement across an entire layer for closed cross-sectional shapes, within the robot's operational range. The second challenge



Figure 1 Aluminum mullions used in architectural facades

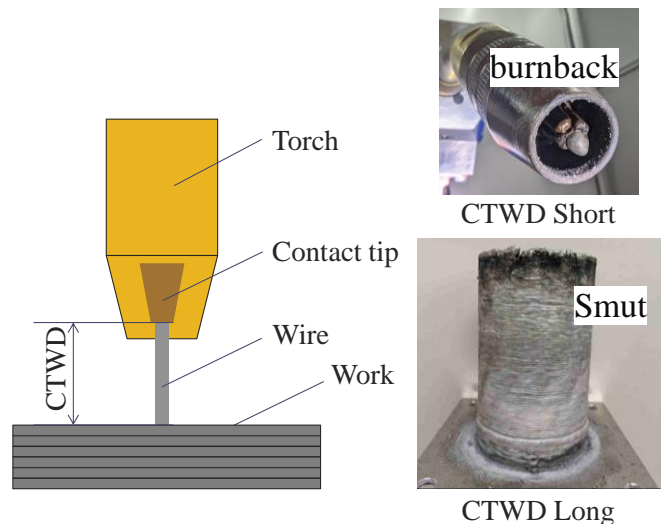


Figure 2 Definition of Contact Tip to Work Distance (CTWD) and associated issues

is the variability in the thickness of the workpiece. When fabricating elongated workpieces using WAAM, the path length per layer is short. In this case, heat accumulation tends to dominate over cooling during deposition, leading to excessive thickness from continuous deposition [16]. This can lead to unnecessary material use, increasing material costs and the weight of the workpiece. Therefore, cooling needs to be implemented, and interpass temperatures must be controlled to stabilize the bead thickness. Additionally, void formation is a major issue in aluminum welding [17], [18]. WAAM samples manufactured at high interpass temperatures have shown fewer voids compared to those produced at lower temperatures [19], indicating that interpass temperature control is critical for improving the quality of the workpiece. Interpass temperature measurement methods can be broadly divided into contact and non-contact methods. Given the changing shapes of workpieces in additive manufacturing, using a contact thermometer is deemed inappropriate. Therefore, a thermographic camera was chosen for measuring the interpass temperature, which allows for the non-contact and two-dimensional visualization of temperature distribution.

In light of the above considerations, the objective of this study is to present a control rule that enables the control of CTWD and interpass temperature during WAAM fabrication and to verify its effectiveness. For this purpose, a trial was conducted to fabricate a full-length 3300 mm aluminum mullion with a hexagonal cross-section. The existing WAAM equipment configuration did not allow for the single-piece fabrication of a 3300 mm mullion due to the limited range of motion. Therefore, the mullion was divided into four parts for the fabrication test. The fabricated mullion parts were analyzed using X-ray CT scanning for thickness analysis and internal defect analysis, confirming the effectiveness of the proposed control rule.

2. Closed-Loop Process Control System

Fabrication strategy incorporating control of both CTWD and interpass temperature was considered. The configuration of the fabrication equipment includes a 6 Degrees Of Freedom (DOF) robot arm, a single-axis positioner table, a laser profiler, and a thermographic camera. The fabrication strategy discussed here, applicable to any workpiece where each layer forms a closed curved surface, is shown in Figure 3. The process involves first continuing deposition for N layers, where N is any integer, following a pre-determined torch path on a feed-forward basis. Afterward, deposition is paused to allow natural cooling of the workpiece and to prevent heat accumulation. Furthermore, by conducting measurements during arc stoppage, various sensors can avoid disturbances caused by arc light. Once the deposition is paused, the robot arm fitted with the laser profiler measures the cross-sectional shape of the layer just deposited before the pause. To extract features such as the height and thickness of the workpiece from the measurement results, the measurement line of the laser profiler is aligned perpendicular to the tangent of the torch path, as shown in Figure 4. This alignment is done for the layer deposited just before the stoppage. To measure the full area of the layer just deposited before the pause, the positioner table rotates one full turn around its axis. Meanwhile, the robot moves the laser profiler's measurement line to intersect the torch path in the x -direction. Additionally, the robot rotates the laser profiler by an angle θ with respect to the x -axis. Using the rotation of the positioner table, it is possible to perform measurements over the entire circumference of a layer within the range of motion of the robot. After the measurements are completed, the average error of the CTWD from the target value in the layer just deposited is calculated, and this average error is corrected in the torch path for subsequent layers. Then, the interpass temperature near the point of resuming deposition is measured by the thermographic camera mounted on the deposition robot, and deposition is resumed once the

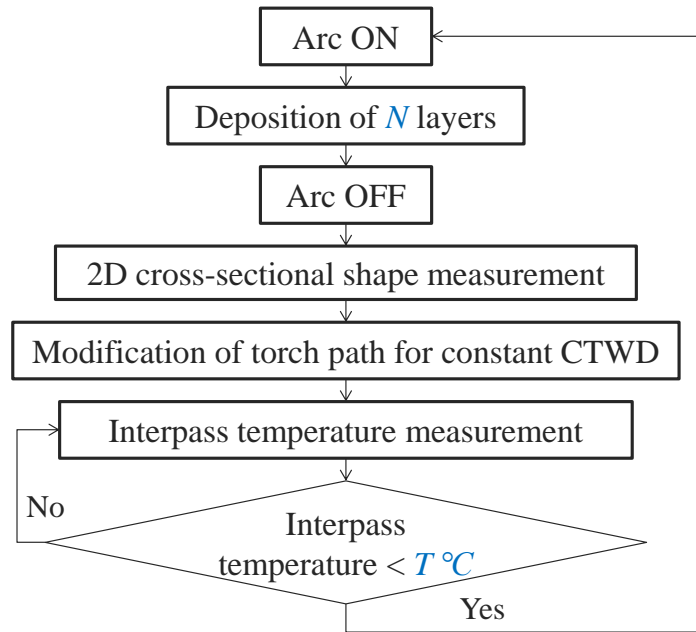


Figure 3 Control flow during fabrication

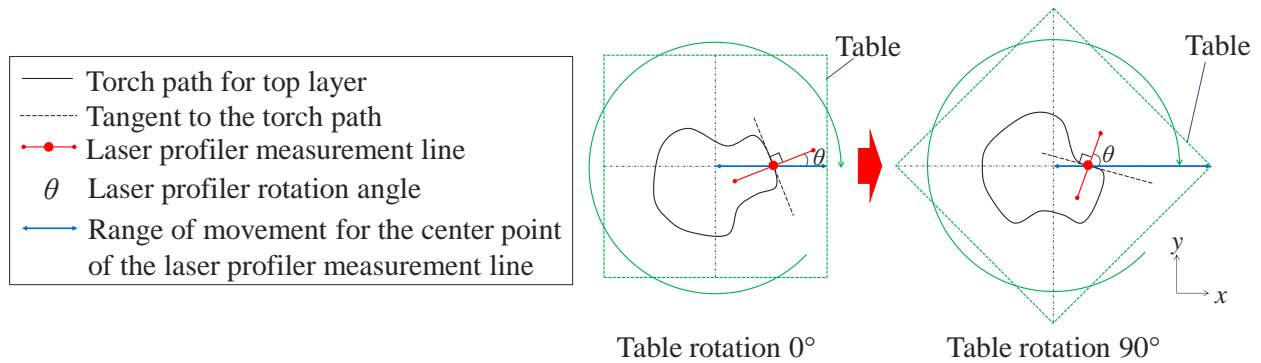


Figure 4 Position of the laser profiler during 2D cross-sectional shape measurement

temperature falls below the threshold T °C. This closed-loop is repeated until the fabrication is complete, keeping the CTWD and interpass temperature within a specified range. If N , the number of continuous layers, is large, the CTWD error may increase. If N is small, the error in CTWD decreases, but more time is spent on measurements and cooling. Thus a balance between fabrication accuracy and time must be considered in deciding N .

3. Trial Fabrication

3.1 Target Mullion Shape

The mullion shape targeted for fabrication in this study is shown in Figure 5. It is a hollow structure 3300 mm in length with a hexagonal cross-section that twists along its height, which would be difficult to manufacture using traditional aluminum forming methods such as machining or casting. Due to the limitations of the robot's range of motion in commonly available WAAM equipment, it is challenging to fabricate a full-length 3300 mm mullion in one piece. Therefore, as shown in Figure 5, the mullion was divided into four parts for fabrication, and after fabrication,

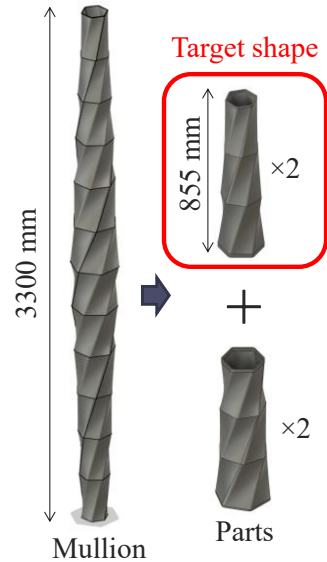


Figure 5 Shape of the target mullion for fabrication and its segmented parts.

each part was joined to assemble the complete mullion. Since the mullion has a symmetrical structure above and below, two identical mullion parts are fabricated and joined together. This paper summarizes the results of fabricating the narrower of the two types of mullion parts.

3.2 Conditions for Fabricating the Mullion Parts

The WAAM fabrication of mullion parts was carried out using a configuration shown in Figure 6, which included a 6 DOF industrial robot arm (Yaskawa Electric, MOTOMAN-AR1440)

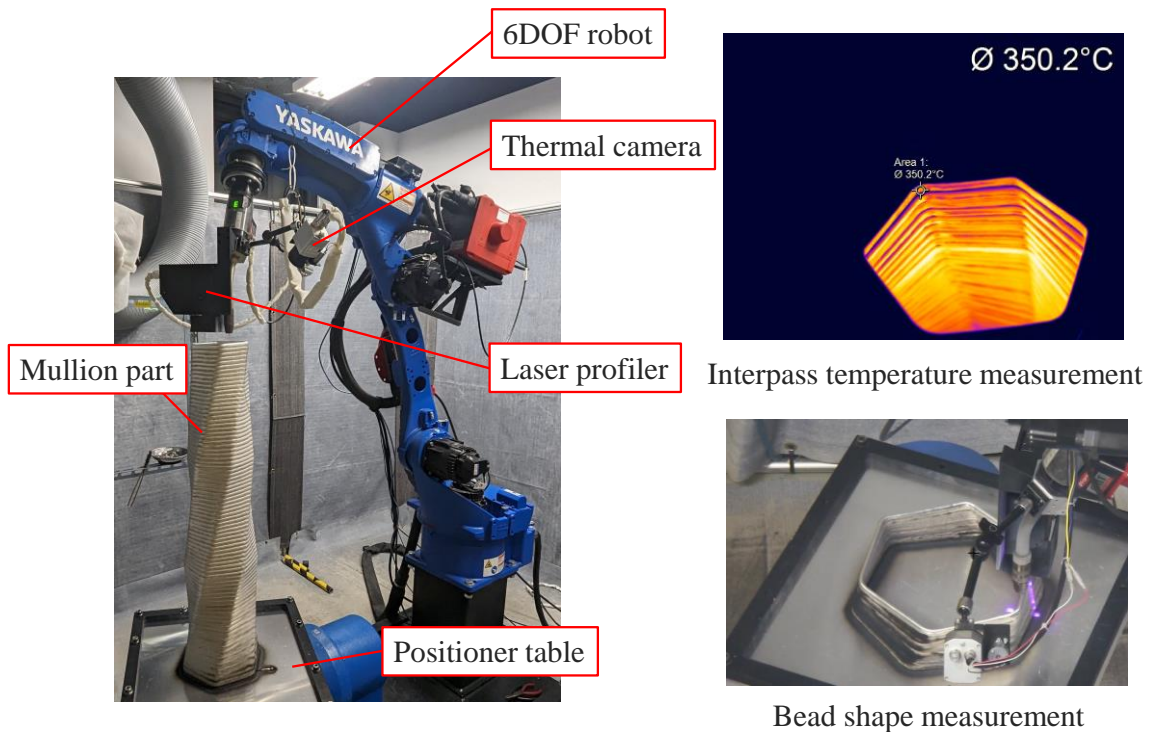


Figure 6 Equipment for mullion parts fabrication

and a CMT welding power source (Fronius, TPS400i). The robot arm was equipped with a laser profiler (Keyence, LJ-V7200 and LJ-X8000A) capable of measuring two-dimensional cross-sections, and a thermographic camera (Optris, PI640i) capable of measuring the surface temperature of the workpiece. The conditions for the mullion parts' fabrication are listed in Table 1. The fabrication used 1.2 mm A5356 aluminum welding wire, A5052 as the substrate, and 99.9 % argon gas as the shielding gas. The first layer alone was deposited using pulsed welding, and subsequent layers were deposited using CMT at a consistent wire feed speed. The torch travel speed was adjusted according to the height of the workpiece. A higher heat input per unit length was set for the initial layers, where the influence of heat dissipation from the substrate is significant. A continuous layer number $N = 10$ and an interpass temperature threshold $T = 350$ °C were set. The torch was always positioned vertically downward during deposition, and the torch path was a spiral that ascended 1 mm per layer around the table's rotational axis.

3.3 Results and Discussion

Using the fabrication method that incorporated control of both CTWD and interpass temperature, it was possible to automatically fabricate mullion parts with a height of 855 mm. This contributes to eliminating costs such as trial and error for height path adjustment and monitoring work during fabrication. The workpiece height and the deposition height pitch per 10 layers, measured from the robot coordinates, are shown in Figure 7. The interpass temperatures measured by the thermographic camera every 10 layers are shown in Figure 8. Two identical mullion parts were fabricated on different days and distinguished as No. 1 and No. 2, both showing similar trends.

Table 1 Fabrication conditions for mullion parts

Parameters	Values
Material	
Welding wire / Substrate	A5356 / A5052
Ar gas flow rate	25 L/min
Welder settings	
1st layer / Pulse : Wire Feed Speed	6.4 m/min
1st layer / Pulse : Current	90 A
1st layer / Pulse : Voltage	13.2 V
2nd -layer / CMT : Wire Feed Speed	6.0 m/min
2nd -layer / CMT : Current	82 A
2nd -layer / CMT : Voltage	12.8 V
Torch travel speed	
0 - 90 mm height	720 mm/min
90 - 178 mm height	720-1200 mm/min
178 mm - height	1200 mm/min
Process parameters	
Number of consecutive layers N	10
Interpass temperature threshold T	350 °C

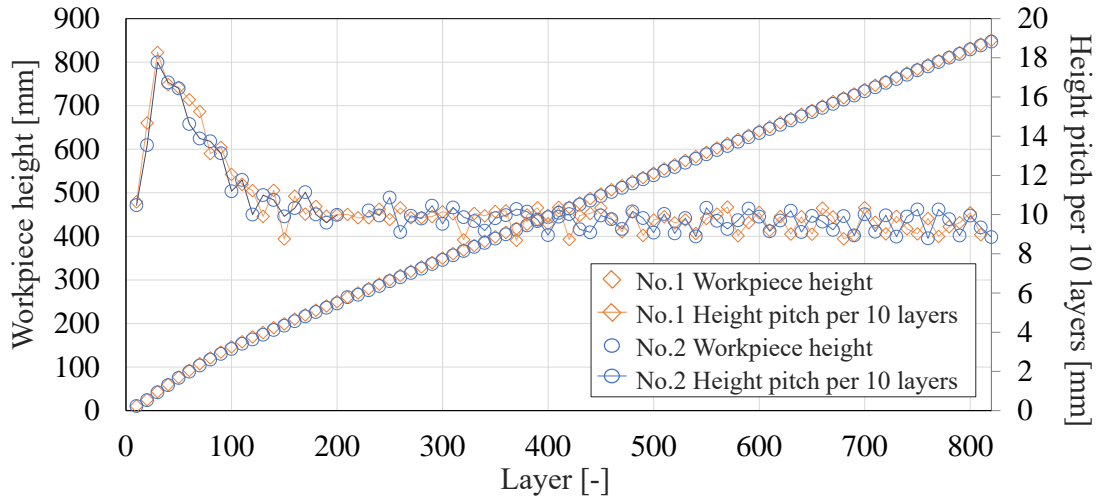


Figure 7 Workpiece height and deposition height pitch per 10 layers

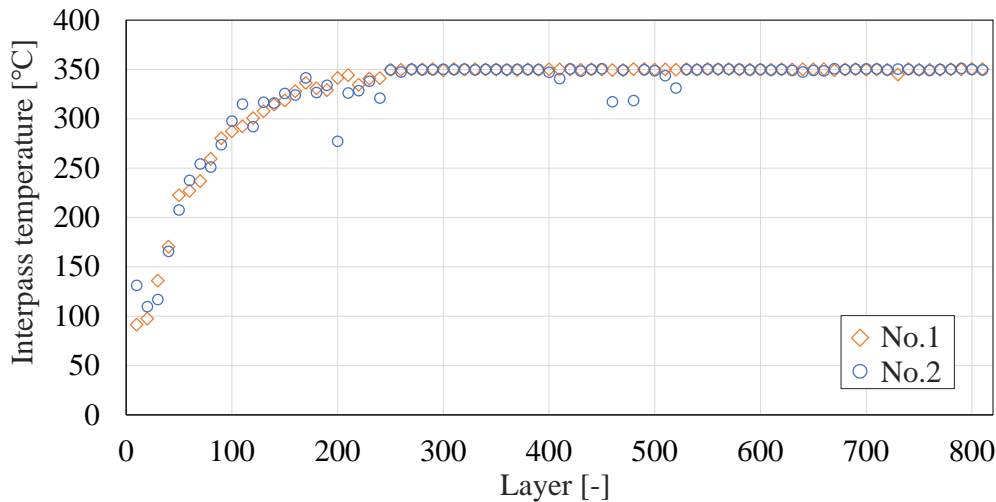


Figure 8 Interpass temperatures measured every 10 layers

In the region below a workpiece height of 178 mm (approximately 130 layers), the heat input per unit length and interpass temperatures varied significantly. Consequently, there was a notable change in the height pitch of the workpiece, indicating the effectiveness of closed-loop control of CTWD. In regions with over 200 layers, where the amount of heat input per unit length was constant and the interpass temperature was maintained at approximately 350 °C, the height pitch of the workpiece stabilized. Therefore, the interpass temperature control effectively stabilized the height and thickness of the bead.

The total time required to fabricate one part was 10.2 hours, of which 6.3 hours was for deposition and 3.9 hours was for measurement and cooling. Therefore, for example, if the number of consecutive layers is set to $N = 5$ to double the frequency of measurement, measurement and cooling time may take longer than deposition time. Therefore, it is necessary to set N appropriately considering the trade-off between build accuracy and build time.

4. Thickness Analysis and Internal Void Analysis of the Mullion Parts

4.1 Measurement Method

Thickness variability, characteristic of WAAM, was observed in the mullion parts. The presence of internal voids, a common issue in aluminum welding, was also a concern. Therefore, X-ray CT scanner (Nikon C2) was used to acquire the shapes of three sections along the height of the mullion parts, and these shapes were combined using VGSTUDIO (Volume Graphics). The combined shape data was used for thickness analysis using the ray method [20] and internal void analysis in VGSTUDIO. The resolution of the data was 156 μm /voxels.

4.2 Results and Discussion

The histogram of the thickness distribution calculated from the thickness analysis results and its normal distribution are shown in Figure 9. Although the thickness distribution closely resembles a normal distribution, the peak is shifted towards the right. This deviation is likely attributed to the shorter path length per layer and the higher interpass temperature in upper layers. These factors tend to increase the thickness of the deposited material. The two mullion parts, No.1 and No.2, were fabricated on different days, but the distribution trends were similar. The difference in average thickness between the two parts was only 0.09 mm, demonstrating high reproducibility. Thus, the feedback control of height and interpass temperature control ensured the reproducibility of the thickness distribution.

The results of the internal void analysis are shown in Figure 10. A total of three voids were identified in No.1, and two voids were found in No.2. In all cases, voids occurred directly above the areas where the irregularities were observed, as shown in Figure 10. These irregularities were caused by a robot operation failure. This failure occurred due to packet loss during UDP communication used to transmit command values from the PC to the robot controller. As a result, the robot reverted to a previous command position, leading to double-layering in certain areas. This issue can be prevented by switching to TCP communication. The occurrence of voids was a concern at locations where layering resumed every 10 layers due to the instability of bead shape at the start of welding. However, no voids were detected near the 81 resumption points of each column. Therefore, it is inferred that the heat input conditions and interpass temperatures were appropriately configured, thus preventing the formation of internal voids.

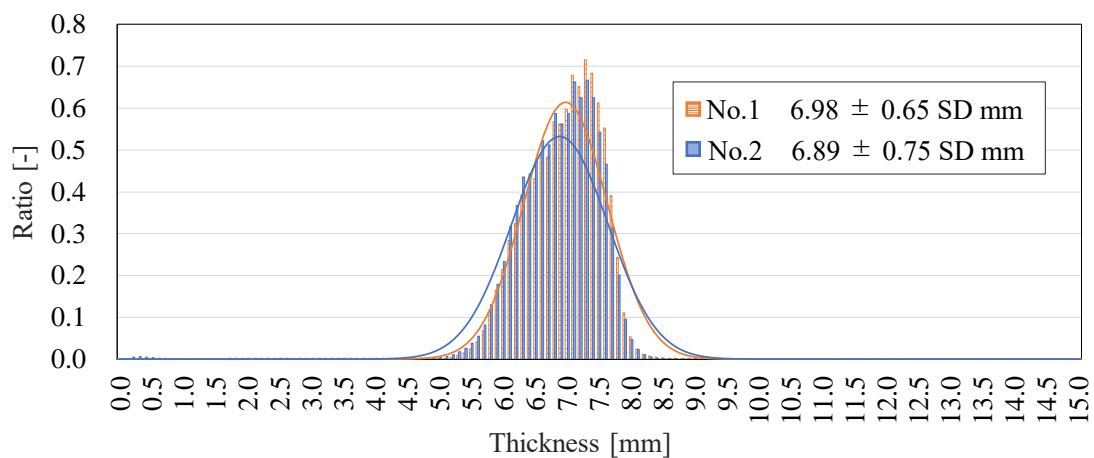


Figure 9 The thickness distribution of the mullion parts and its normal distribution

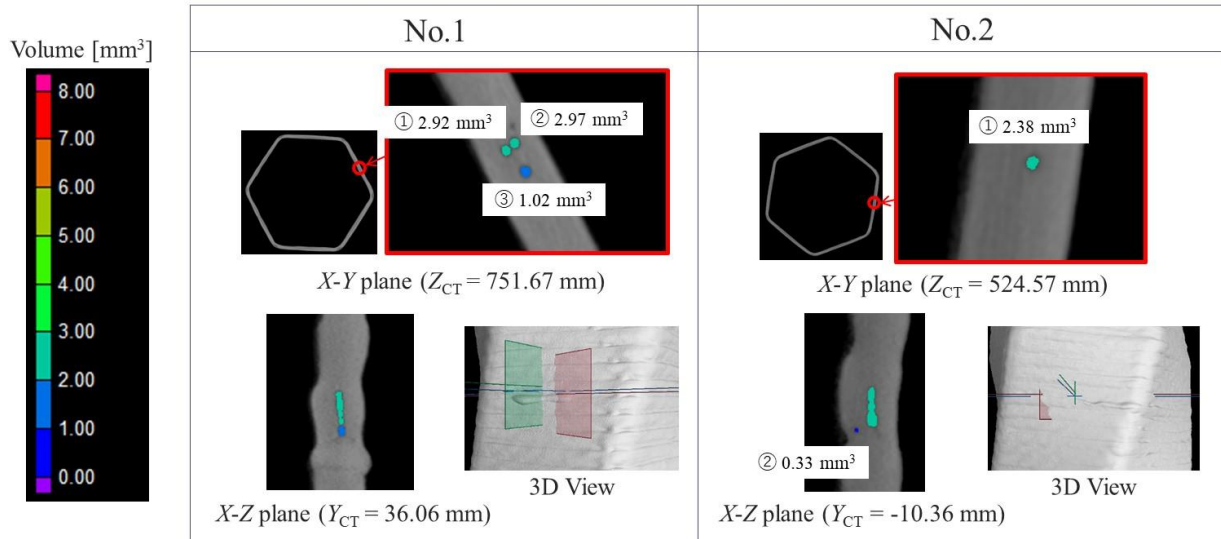


Figure 10 Voids present in the mullion parts

5. Conclusion

In this study, we explored the fabrication methods for architectural facades ranging from 3 to 5 meters using WAAM, focusing on the automatic construction of aluminum mullion parts with a height of 855 mm. We presented a control rule that enabled the management of CTWD and interpass temperature during the WAAM process and verified its effectiveness through trials. The fabricated mullion parts were subjected to X-ray CT scanning to obtain their shape and were analyzed for thickness distribution and internal voids. The results confirmed the following:

- (1) The introduction of CTWD and interpass temperature control in the fabrication method allowed for the successful automatic manufacturing of a mullion part measuring 855 mm in height.
- (2) The closed-loop control of CTWD proved particularly effective in the initial layers, where the heat input per unit length and interpass temperature varied significantly.
- (3) The control of CTWD and interpass temperature ensured the reproducibility of the thickness distribution in the workpiece.
- (4) The interpass temperature control was instrumental in suppressing void formation upon deposition resumption points

Therefore, the CTWD and interpass temperature control system developed in this study contributes to the automation and quality stabilization of aluminum facade components' manufacturing.

References

- [1] I. Caetano, L. Santos, and A. Leitão, “Computational design in architecture: Defining parametric, generative, and algorithmic design”, *Frontiers of Architectural Research*, Vol. 9, Issue. 2, pp. 287–300, 2020.
- [2] C. Bañón and F. Raspall, “3D Printing Architecture: Workflows, Applications, and Trends”, *Springer*, 127pp, 2021.
- [3] V. S. Fratello and R. Rael, “Innovating materials for large scale additive manufacturing: Salt, soil, cement and chardonnay”, *Cement and Concrete Research*, Vol. 134, 2020.
- [4] J. Pasco, Z. Lei, and C. Aranas, Jr, “Additive Manufacturing in Off-Site Construction: Review and Future Directions”, *Buildings*, Vol. 12, No. 53, 2022.
- [5] C. Buchanan and L. Gardner, “Metal 3D printing in construction: A review of methods, research, applications, opportunities and challenges”, *Engineering Structures*, Vol. 180, pp. 332–348, 2019.
- [6] J. Lange, T. Feucht, and M. Erven, “3D-Printing with Steel - Additive Manufacturing for connections and structures”, *Steel Construction*, Vol. 13, Issue. 3, pp. 144–153, 2020.
- [7] W. Jin, C. Zhang, S. Jin, Y. Tian, D. Wellmann, and W. Liu, “Wire Arc Additive Manufacturing of Stainless Steels: A Review”, *Applied Sciences*, Vol. 10, Issue. 5, 2020.
- [8] A. Garcia-Colomo, D. Wood, F. Martina, and S. W. Williams, “A comparison framework to support the selection of the best additive manufacturing process for specific aerospace applications,” *International Journal of Rapid Manufacturing*, Vol. 9, No. 2–3, pp. 194–211, 2020.
- [9] S. W. Williams, F. Martina, A. C. Addison, J. Ding, G. Pardal, and P. Colegrove , “Wire + Arc Additive Manufacturing”, *Materials Science and Technology*, Vol. 32, Issue. 7, 2016.
- [10] C. B. Costanzi, B. Waldschmitt, U. Knaack and J. Lange, “Transforming the Construction Industry Through Wire Arc Additive Manufacturing”, *SpringerLink*, pp. 213-238, 2023.
- [11] S. Kesawan, M. Mahendran, and B. Baleshan, “Section moment capacity tests of complex-shaped aluminium mullions”, *Thin-Walled Structures*, Vol. 131, pp. 855–868, 2018.
- [12] Y. Sugiyama, J. Nakata, and H. Miyauchi, “Reducing smut in aluminium alloy welds using double wire MIG (DWM) welding”, *Welding International*, Vol. 7, Issue. 3, pp. 177-182, 2009.
- [13] L. V. Hölscher, T. Hassel, H. J. Maier, “Development and evaluation of a closed-loop z-axis control strategy for wire-and-arc-additive manufacturing using the process signal”, *The International Journal of Advanced Manufacturing Technology*, Vol.128, pp.1725-1739, 2023.
- [14] M. Baldauf, P. Lohrer, T. Hauser, L. Jauer and J. H. Schleifenbaum, “Camera-based measurement and control of the contact tip to work distance in wire arc additive manufacturing”, *Progress in Additive Manufacturing*, Vol.9, pp. 565-574, 2024.
- [15] R. T. Reisch, T. Hauser, J. Franke, F. Heinrich, K. Theodorou, T. Kamps, and A. Knoll, “Nozzle-to-Work Distance Measurement and Control in Wire Arc Additive Manufacturing.” *Proceedings of the 2021 European Symposium on Software Engineering*, pp. 163–172, 2022.
- [16] A. Scotti, “The Potential of IR Pyrometry for Monitoring Interpass Temperature in Wire + Arc Additive Manufacturing”, *Evolutions in Mechanical Engineering*, Vol. 3, Issue. 1, 2019.
- [17] D. Ardika, T. Triyono, N. Muhayat, and Triyono, “A review porosity in aluminum welding”, *Procedia Structural Integrity*, Vol. 33, pp. 171–180, 2021.
- [18] M. Arana, E. Ukar, I. Rodriguez, A. Iturrioz and P. Alvarez, “Strategies to Reduce Porosity in Al-Mg WAAM Parts and Their Impact on Mechanical Properties”, *Metals*, Vol.11, Issue. 3, 2021.

- [19] K. Derekar, J. Lawrence, G. B. Melton, A. Addison, X. Zhang, and L. Xu, “Influence of Interpass Temperature on Wire Arc Additive Manufacturing (WAAM) of Aluminium Alloy Components”, *MATEC Web Conferences*, Vol. 269, 2019.
- [20] “Spheres and Rays: Wall Thickness Analysis”, *Volume Graphics*, Accessed: Jun. 14, 2024, <https://www.volumegraphics.com/en/stories/spheres-and-rays-wall-thickness-analysis.html>.